

## Actual microstructure-based numerical method for mesomechanics of concrete

S. Chen<sup>a</sup>, Z.Q. Yue<sup>b</sup> and A.K.H. Kwan<sup>\*</sup>

*Department of Civil Engineering, The University of Hong Kong, Pokfulam Road, Hong Kong, China*

*(Received October 1, 2009, Revised April 22, 2011, Accepted December 6, 2011)*

**Abstract.** This paper presents an actual microstructure-based numerical method to investigate the mechanical properties of concrete at mesoscopic level. Digital image processing technique is used to capture the concrete surface image and generate the actual 3-phase microstructure of the concrete, which consists of aggregate, matrix and interfacial transition zones. The microstructure so generated is then transformed into a mesh or grid for numerical analysis. A finite difference code FLAC2D is used for the numerical analysis to simulate the mechanical responses and failure patterns of the concrete. Several cases of concrete with different degrees of material heterogeneity and under different compression loading conditions have been analysed. From the numerical results, the effects of the internal material heterogeneities as well as the external confining stresses are studied. It is shown that the material heterogeneities arising from the presence of different phases and the existence of interfacial transition zones have great influence on the overall mechanical behaviour of concrete and that the numerically simulated behaviour of concrete with or without confining stresses applied agrees quite well with the general observations reported in the literature.

**Keywords:** digital image processing; interfacial transition zones; mesomechanics

---

### 1. Introduction

Like other geomaterials, concrete is a material with a variety of heterogeneities. At mesoscopic level, it is considered as a 3-phase material consisting of coarse aggregate, mortar matrix, and interfacial transition zones (Zaitsev and Wittmann 1981, Wriggers and Moftah 2006, Comby-Peyrot *et al.* 2009). The material microstructure has great effects on the internal stress/strain distributions and therefore governs the failure characteristic of the concrete. As a result, the structural performance of concrete at engineering level is closely related to the mechanical properties of the concrete at mesoscopic level. For years, extensive investigations have been carried out by means of laboratory testing, theoretical analysis and numerical modelling to examine the mesoscopic mechanical behaviour of concrete. Among the various means, numerical modelling with the material heterogeneities incorporated for mechanical analysis is the most

---

\*Corresponding author, Professor, E-mail: khkwan@hku.hk

<sup>a</sup>Ph.D. Student

<sup>b</sup>Associate Professor

generally applicable and effective. There are two major steps in the numerical modelling. First, it is necessary to generate the 3-phase microstructure of the concrete for mechanical analysis. Then, the mechanical behaviour of the heterogeneous concrete is analysed by a suitable numerical method.

One method of generating the microstructure of concrete is to generate statistically the random aggregate structure based on known or assumed size, shape and spatial distributions of the coarse aggregate particles. From the aggregate structure, the mortar matrix is generated as the interstitial space between the coarse aggregate particles, and the interfacial transition zones are generated as the boundaries between the coarse aggregate and mortar matrix. Researchers adopting this method include Wittmann *et al.* (1984), Bazant *et al.* (1990), De Schutter and Taerwe (1993), Wang *et al.* (1999) and Kwan *et al.* (1999b). They used various approaches to generate the random aggregate structure and different numerical methods to analyse the mechanical behaviour of the heterogeneous concrete. Specifically, Wang *et al.* (1999) and Kwan *et al.* (1999b) have jointly developed a method of putting the aggregate particles one by one into the volume of concrete to generate the random aggregate structure and used the finite element method to simulate the propagation of cracks in concrete under direct tension.

Another method of generating the microstructure is to employ a lattice model, in which the members are assigned material properties corresponding to those of the aggregate, matrix or interfacial transition zones, according to the phase into which the individual member falls. Schlangen and Van Mier (1992) were the first to develop such a model. They used a regular lattice and generated the microstructure either manually or by a random generator. With this lattice model, they simulated the propagation of tension cracks in concrete under shear by performing elastic analysis of the lattice and removing any member that has failed. Schlangen and Garboczi (1996) further developed the lattice model by using a random lattice instead of a regular one. Raghuprasad *et al.* (1998) also adopted the lattice model, but instead of removing the failed members, eliminated the stresses in the failed members by applying appropriate nodal forces. Using this method, they have studied the behaviour of concrete under direct tension. Later, Leite *et al.* (2007) extended this method to 3-dimensional modelling and Rempling and Grassl (2008) applied this method to study concrete subjected to cyclic compression.

More recently, Zhu *et al.* (2004) have developed a method of generating the microstructure of concrete using a regular finite element mesh, in which the elements are assigned material properties as per the phase that the individual element is intended to model, in a way similar to the lattice model. The microstructure of the concrete is represented by domain groups of elements modelling the aggregate particles, which are arbitrarily generated by hand on the computer screen. A single layer of elements surrounding each aggregate particle is automatically identified to model the interfacial transition zone. The random variations of the material properties within each phase are also simulated. With this finite element model, they have analysed the mesoscopic mechanical behaviour of concrete under shear, tension and compression.

Apart from the above, other analysis methods have also been employed. For instance, some researchers have successfully applied the finite difference method, through the use of the computer code FLAC (ITASCA 1995), to study the composite behaviour of heterogeneous materials, such as rock and concrete, as exemplified by the papers published in the Second International FLAC Symposium (Billaux *et al.* 2001). On the other hand, Azevedo *et al.* (2002) have generated the microstructure of concrete as a random package of circular particles bonded together by mortar matrix and simulated the fracture behaviour of concrete under shear and tension using the discrete element method, which deals with the analysis as a multiple contact problem.

Through the many years of effort in generating the microstructure of concrete and simulating the mechanical behaviour of the 3-phase composite material under various loading conditions, our understanding of the mesoscopic behaviour of concrete has advanced greatly. However, it should be noted that the microstructures acquired for analysis in the previous studies were all artificial structures generated either arbitrarily by hand or randomly by statistical tools. There are up to now no or very few publications in the literature providing information on how the artificially generated microstructures compare to the actual microstructures of concrete with different mix compositions. Considering the lack of proof of the validity of the artificially generated microstructures, the reliability of the existing models in revealing the mesoscopic behaviour of real concrete may be questionable. It is felt that studies based on the actual microstructures of representative samples should produce more reliable results.

Aiming at establishing the actual microstructures of multi-phase geomaterials for analysing how the internal structures would affect the overall behaviour, Yue *et al.* (2003a, b) and Chen *et al.* (2004a, b) have jointly developed a digital image-based numerical modelling method of capturing the actual microstructure of the material for analysis. This method employs the digital image processing technique to extract the spatial information of the various components in the geomaterial from digital images of the surfaces or cross-sections of the geomaterial. The spatial information is then transformed into a mesh or grid for incorporation into traditional numerical methods to investigate the mechanical responses and failure modes of the geomaterial under different loading conditions. This digital image-based modelling method has been successfully applied to rock, soil and asphalt concrete.

In this paper, we extend the digital image-based numerical modelling method to study cement concrete. The digital image processing technique is employed to capture images from concrete samples and generate the actual microstructures of the concrete. A finite difference code is then used to simulate the crack propagation process in concrete under different compression loading conditions. The numerical results show very clearly that the material heterogeneities play an important role in determining the mechanical behaviour of concrete under uniaxial or triaxial compression loads.

## 2. Digital image processing

### 2.1 Basic concepts

Digital image processing is concerned with the transformation of an optical image of the scene under study into a digital data format and the computer processing of the digital data so acquired to produce useful information, such as the number, size, shape and relative positions of the various objects appearing in the scene. There are two basic steps: image acquisition and image processing.

During image acquisition, the optical image of the scene is captured and digitised for storage. The image is divided into small regions called pixels, which are usually arranged in a rectangular grid. To capture the image, the brightness or colour of each pixel is scanned sequentially. The electronic signal from the sensor is then digitised by an analogue-to-digital converter for storage into two-dimensional arrays of discrete numbers representing the brightness or colour of the pixels. For example, a colour image can be digitised into three arrays, each representing the intensity of the red, green and blue colour of the image, as shown in the following equation, where  $M$  and  $N$  are the number of pixels in the  $i$  and  $j$  Cartesian coordinate, and  $k$  ranges from 1 to 3,

each for one colour

$$f_k(i, j) = \begin{bmatrix} f_k(1,1) & f_k(1,2) & \cdots & f_k(1,N) \\ f_k(2,1) & f_k(2,2) & \cdots & f_k(2,N) \\ \vdots & \vdots & & \vdots \\ f_k(M,1) & f_k(M,2) & \cdots & f_k(M,N) \end{bmatrix} \quad (1)$$

In this study, a digital scanner is used for image acquisition. Fig. 1 shows the colour image of a cross-section of cement concrete made with granite aggregate. The physical size of the concrete section is 25.83 mm  $\times$  48.25 mm while the resolution of the digitised image is 243  $\times$  454. Hence, the physical size of each pixel is 0.106 mm  $\times$  0.106 mm.

During image processing, the digital image (the arrays of numbers representing the brightness or colour of the pixels) is processed to identify objects in the scene for detailed study and to extract useful information about the identified objects. Many different algorithms and techniques have been developed for image processing. In this project, a software package called MATLAB (The MathWorks Inc. 2007) is employed. MATLAB, which stands for matrix laboratory, contains a digital image toolbox and plenty of image processing functions for a wide range of applications.

With the rapid development of electronic camera, computer hardware and image processing software, digital image processing has exhibited tremendous growth and exerted a great impact in many disciplines, including medical science, biology, aviation, production industry and civil engineering. Due to limited space in this paper, only several successful applications of digital image processing to geomaterials, such as those by Yue and Morin (1996), Mora *et al.* (1998), Kwan *et al.* (1999a), Mora and Kwan (2000), Chermant (2001) and Chermant *et al.* (2001), are cited here. Most of these studies employed the digital image processing techniques to analyse the geometry and spatial distributions of the various ingredients in asphalt and cement concrete.

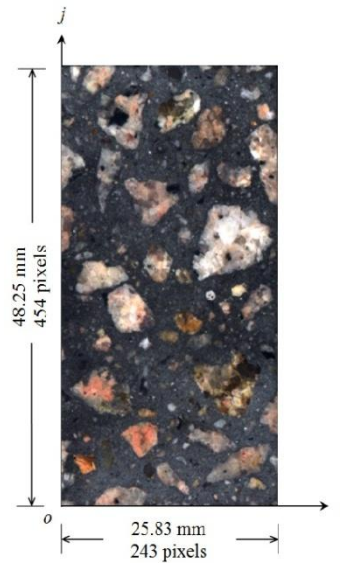


Fig. 1 Colour image of cement concrete surface

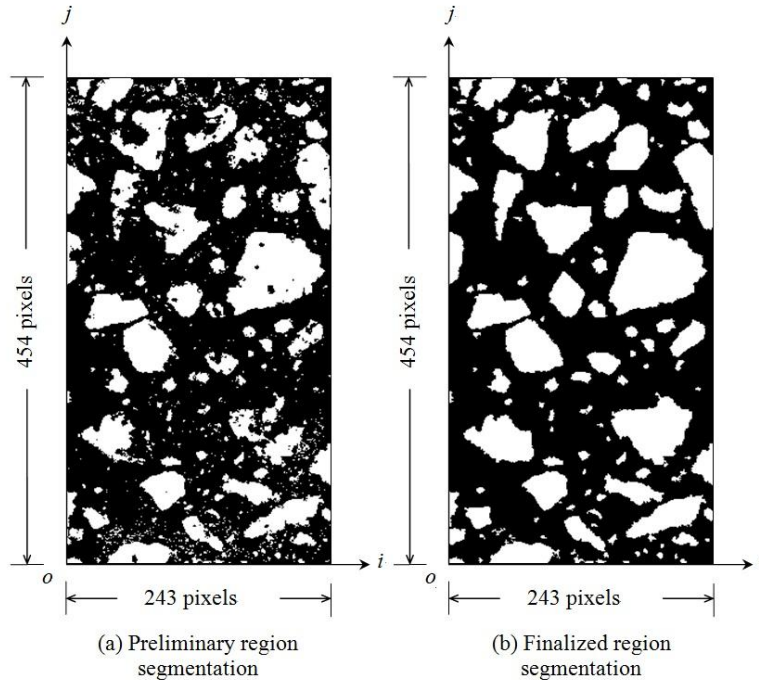


Fig. 2 Digital image processing to establish material heterogeneity

## 2.2 Establishment of material heterogeneity

From the variations in grey level or colour, image processing can detect the presence of different objects/materials and pick up the details of individual features. Basically, two different approaches, namely, region segmentation method and edge detection method, can be employed to identify individual object/material from the digital image. The region segmentation method partitions the image into disjoint regions by finding the areas with similar grey level or colour attributes. The edge detection method separates the image into disjoint regions by finding the boundaries where there are sharp changes in grey level or colour attributes. Chen *et al.* (2004b) have used a multi-threshold region segmentation method to detect the presence of certain minerals in granite rock. Herein, this same technique is adopted to detect the presence of aggregate particles in cement concrete and partition the concrete area into aggregate and matrix.

Apart from the RGB colour system (R, G and B stand for red, green and blue), the colour of each pixel may also be described in terms of the HSI colour system (H, S and I stand for hue, saturation and intensity), which is an important colour space in human vision. The HSI values of each pixel can be obtained easily from the corresponding RGB values using an image processing function in MATLAB. Our experience in digital image processing of cement concrete made with granite aggregate indicated that the I-values of the aggregate particles are usually higher than those of the cement matrix. Hence, the aggregate particles may be distinguished from the cement matrix by checking whether the I-values of the pixels are higher than a certain threshold value. In this study, a threshold value of 0.4 is adopted. In other words, if the I-value is lower than 0.4, the pixel is taken to be part of the matrix phase and if otherwise, the pixel is taken to be part of the

aggregate phase. Fig. 2(a) shows the preliminary region segmentation so obtained from the concrete image in Fig. 1, with the matrix phase depicted in black and the aggregate phase depicted in white to increase the contrast between the two phases.

One can see that in Fig. 2(a), there are some black clumps in the white areas and many small white clumps in the black areas. The black clumps in the white areas are in reality spots of dark colour minerals in the granite rock rather than inclusions of matrix within the aggregate phase. These black clumps should have been part of the aggregate phase and are thus removed from the image using a standard function in MATLAB. On the other hand, the small white clumps in the black areas are fine aggregate particles. Since in mesoscopic studies, only the coarse aggregate particles are considered as constituting the aggregate phase and the fine aggregate particles are considered as part of the mortar matrix phase, we can focus on the relatively large aggregate particles by removing the small aggregate particles from the image. In this study, an aggregate particle in the digital image is regarded as small if the number of pixels representing it is equal to or smaller than 10 (the physical area of 10 pixels is equal to  $10 \times 0.106 \text{ mm} \times 0.106 \text{ mm} = 0.112 \text{ mm}^2$ ). All such small aggregate particles are removed from the image using a standard function in MATLAB. Lastly, some minor revisions of the region segmentation are performed via the Windows Painter software by comparing the region segmentation result with the real concrete sample. The finalised region segmentation is shown in Fig. 2(b).

### 2.3 Generation of microstructure for analysis

In most numerical methods, such as the finite element method and the finite difference method, the material domains have to be discretised using a suitable discretisation scheme into many small elements in the form of a mesh or many small areas in the form of a grid. However, in a digital image of concrete, an automatic discretisation scheme has already been applied because the digital image is by itself an array of pixels. Each pixel occupies a small spot on the concrete cross-section and so may be considered as either an element in a finite element mesh or an area between finite difference grid lines. Each pixel also represents a certain material and so may be taken as modelling the constitutive material that it represents. A simple data transformation can transform the digital image into a finite element mesh or a finite difference grid modelling the material microstructure of the concrete. Such a material microstructure can be easily incorporated into many existing commercial software products for numerical analysis.

The above microstructure consists of only two phases, namely, aggregate and matrix. However, one obvious characteristic that distinguishes cement concrete from other geomaterials is the existence of the third phase - the interfacial transition zones between aggregate and matrix. It has long been recognised that at the surface of each coarse aggregate particle, there is a thin layer of cement paste, called an interfacial transition zone (ITZ), which is more porous than the bulk cement paste further away from the coarse aggregate. Extensive studies by means of X-ray diffraction, scanning electron microscopy and transmission electron microscopy etc have been carried out to examine the physical structure of the ITZs and it has been found by many researchers, including Oliver *et al.* (1995), Mindess (1996), Diamond and Huang (2001), and Liao *et al.* (2004), that the thickness of an ITZ is generally of the order of 30 to 100  $\mu\text{m}$ . Being the weakest links, the ITZs have great influence on the fracture behaviour of concrete, as revealed by the laboratory observation that a microcrack would generally start at an ITZ before it propagates through the matrix to become a major crack (Scrivener and Pratt 1996, Akcaoglu *et al.* 2005).

To allow for the presence of the ITZs, for each aggregate particle, a single layer of elements

surrounding the aggregate particle is automatically generated as a one element thick interface between the aggregate and matrix phases. In this specific simulation study, the width of each element in Fig. 2 is 0.106 mm, which is very much the same as the ITZ thickness value of 100  $\mu\text{m}$  determined from laboratory tests. Moreover, the conventional wisdom that regards the ITZs as the weakest links in concrete is followed by assigning relatively low modulus and strength values to the mechanical properties of the elements modelling the ITZs.

### 3. Numerical examples

#### 3.1 Method of analysis and parametric studies

The finite difference code,  $\text{FLAC}^{2\text{D}}$  (a two-dimensional version of  $\text{FLAC}$ ), is employed to analyse the uniaxial and triaxial behaviour of concrete under different compression loading conditions.  $\text{FLAC}$ , which stands for Fast Lagrangian Analysis of Continua, is a stress analysis software package based on an explicit time-marching scheme. It is generally quite efficient. Although many thousands of time steps may be needed before the final results for the force-displacement history and failure mode etc are reached, the total computer time required for the type of problems dealt with in this study is usually within several hours.  $\text{FLAC}$  contains a total of nine basic constitutive models, such as the elastic model, Drucker-Prager and Mohr-Coulomb plastic models, and strain-softening and strain-hardening models, etc, for different types of materials.

In the present study, the image data file is imported and transformed into a finite difference grid for analysis using a  $\text{FLAC}$  built-in tool. The finite difference grid so built up for the microstructure

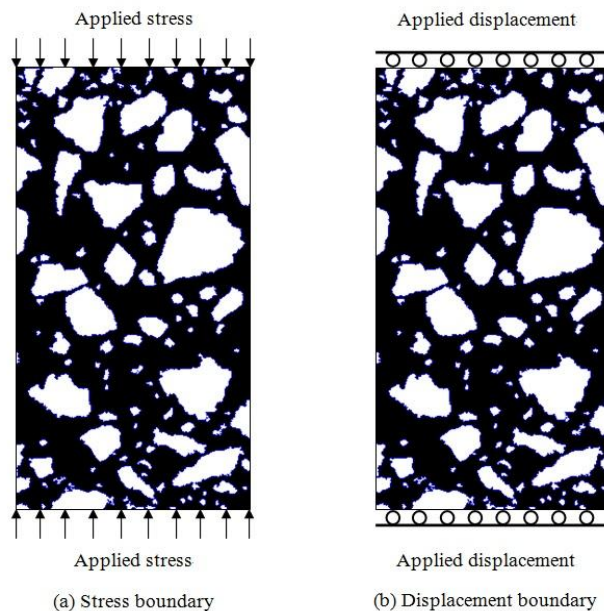


Fig. 3 Boundary conditions applied in the analysis

generated in the previous section contains  $243 \times 454$  square elements, each corresponding to a pixel in the digital image. Having built up the finite difference grid, a material type number is assigned to each element depending on whether it represents the aggregate, matrix or ITZ phase. After then, for each material type, the constitutive model and the corresponding material properties to be used for modelling the constitutive behaviour of the material are entered into the input file.

Whilst working out numerical examples to illustrate the above analysis method, the opportunity is taken to carry out parametric studies to unveil the mesoscopic behaviour of concrete. Three series of parametric studies are carried out. In the first series, the effects of heterogeneity on the stress distribution are investigated by analysing two similar concrete specimens, one homogeneous consisting of a single phase only and the other heterogeneous consisting of the aggregate, matrix and ITZ phases. For this series of study, a stress boundary condition is applied such that prescribed stresses are applied to the two ends of each specimen, as shown in Fig. 3(a).

In the second series, the effects of ITZs on the stress-strain curve and compressive strength are investigated by analysing three similar concrete specimens, one homogeneous consisting of a single phase only, another heterogeneous consisting of the aggregate, matrix and ITZ phases, and the last also heterogeneous but consisting of the aggregate and matrix phases only (no ITZ phase). For this series of study, a displacement boundary condition is applied such that prescribed displacements are applied to the two ends of each specimen, as shown in Fig. 3(b).

In the third series, the effects of confining stresses on the failure pattern, stress-strain curve and compressive strength of the concrete treated as a 3-phase composite material are investigated by analysing concrete specimens with the same actual microstructure but under different confining stresses ranging from 0 to 40 MPa. For this series of study, a displacement boundary condition is applied, as shown in Fig. 3(b).

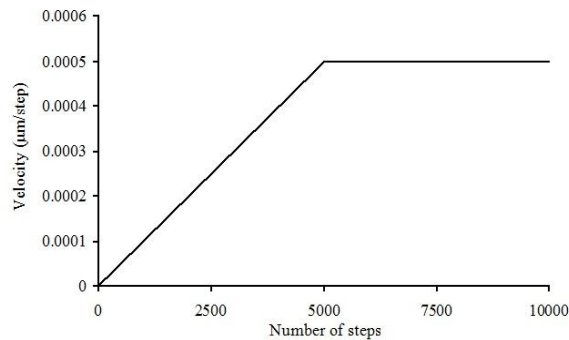
When using FLAC to analyse a geomaterial under prescribed stress or displacement, the prescribed stress can be applied directly in one go but the prescribed displacement has to be applied very slowly and smoothly through many time steps. According to the theory of FLAC, application of any finite increment of prescribed displacement to the boundary would produce a stress wave across the specimen and in order to minimize the induced shock the prescribed displacement has to be applied in a large number of small increments. In the present study, the strategy of controlling the acceleration and velocity of the boundary is adopted. At the start, both the displacement and velocity are set at zero and then a small acceleration is imposed for a given number of time steps. With the small acceleration imposed, the velocity would increase with the number of time steps from zero to a certain maximum value and the corresponding displacement would increase at a rate equal to the velocity. The actual velocity and displacement applied to the ends of the specimen are shown in Fig. 4. As can be seen from the figure, an acceleration of  $1.0 \times 10^{-7} \mu\text{m}/\text{step}^2$  is applied for 5,000 steps until a maximum velocity of  $5.0 \times 10^{-4} \mu\text{m}/\text{step}$  is reached and thereafter the velocity is kept constant until the analysis is completed.

FLAC<sup>2D</sup> is capable of performing two-dimensional analysis under plane stress or plane strain condition. Both the plane stress and plane strain conditions have been considered and applied. The numerical results obtained with the different conditions applied are not quite the same. For brevity, only the numerical results with the plane strain condition applied are presented herein. When studying the effects of lateral confining stresses, the plane strain condition is more appropriate than the plane stress condition because the plane strain condition can help to avoid out-of-plane failure, which tends to occur when in-plane compressive stresses are applied in both directions. In the longer term, 3-dimensional analysis, though much more difficult, should be carried out to take into account the stress/strain applied in the out-of-plane direction.

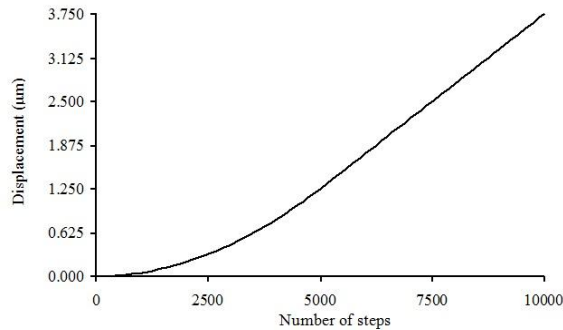
### 3.2 Effects of heterogeneity on stress distribution

The effects of heterogeneity are investigated by analysing the concrete specimen twice, first with the concrete assumed to be homogeneous and then again with the concrete assumed to be heterogeneous consisting of the aggregate, matrix and ITZ phases. A strain-softening constitutive model with tension failure governed by the tensile strength criterion and shear failure governed by the Mohr-Coulomb criterion is adopted for the analysis. In the homogeneous case, all elements in the concrete model are assigned the same material properties taken as the weighted average values of the materials properties of the three individual phases. In the heterogeneous case, each element in the concrete model is assigned the material properties of the phase that it represents. The material properties of the aggregate, matrix and ITZ phases adopted in the heterogeneous case and the weighted average values of these material properties adopted in the homogeneous case are listed in Table 1. These material properties are based on previous experience with typical concrete and the values proposed by Kwan *et al.* (1999b) and Zhu *et al.* (2004). It should be noted that these material properties are assumed typical values solely for the purpose of parametric study. They are not measured values and thus the numerical results of this study cannot be directly compared with any experimental results.

A uniaxial compressive stress of 1 MPa is applied at each end of the concrete specimen as depicted in Fig. 3(a). In the homogeneous case, the numerical results reveal that the vertical



(a) Variation of velocity with number of steps



(b) Variation of displacement with number of steps

Fig. 4 Application of displacement boundary conditions at ends of specimen

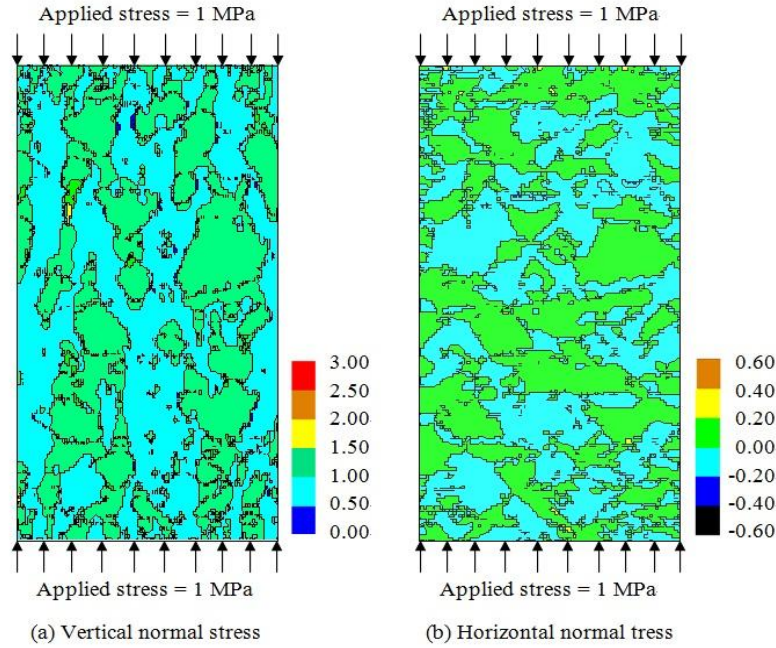


Fig. 5 Effects of heterogeneity on stress distribution (compressive stresses positive)

Table 1 Physical properties and chemical compositions of raw materials

Phase	Elastic modulus(GPa)	Poisson's ratio	Tensile strength(MPa)	Cohesion (MPa)	Friction angle (°)
Aggregate	80.0	0.2	10.0	50.0	50.0
Matrix	25.0	0.2	3.0	40.0	35.0
ITZ	18.0	0.2	1.0	25.0	30.0
Weighted average values of above material properties	43.2	0.2	5.3	42.5	39.8

Note: The weighted average values of the material properties of the aggregate, matrix and ITZ phases are evaluated with the areas occupied by aggregate (33.7%), matrix (60.8%) and ITZ (5.5%) taken as the weighting factors.

normal stresses in all the elements are equal to 1 MPa and the horizontal normal stresses in all the elements are equal to 0 MPa. These results are within expectation and serve to verify the correctness of the analysis. However, in the heterogeneous case, the numerical results reveal that the internal stresses developed are quite irregularly distributed. Fig. 5 plots both the vertical and horizontal normal stresses developed in the concrete in such a heterogeneous case. From the plots for vertical normal stresses, it can be seen that the aggregate phase, which has the highest elastic modulus, is generally subjected to vertical normal stresses higher than 1 MPa. In contrast, the matrix within each gap between adjacent aggregate particles roughly in the same horizontal plane is subjected to vertical normal stresses lower than 1 MPa while the matrix within each gap

between adjacent aggregate particles roughly in the same vertical plane is subjected to vertical normal stresses higher than 1 MPa. On the other hand, from the plots for horizontal normal stresses, it can be seen that although no horizontal normal stresses are applied, horizontal normal stresses are developed inside the concrete. More importantly, both compressive and tensile horizontal normal stresses are developed in the mortar phase and, though not shown in the figure, also in the ITZ phase. Hence, the material heterogeneity has great influence on the internal stress distribution.

### 3.3 Effects of ITZs on stress-strain curve

The effects of ITZs are investigated by analysing the concrete specimen three times, first with the concrete assumed to be homogeneous, second with the concrete assumed to be heterogeneous consisting of the aggregate, matrix and ITZ phases, and third with the concrete assumed to be heterogeneous consisting of the aggregate and matrix phases only. The same strain-softening constitutive model and the same material properties as listed in Table 1 are adopted for the analysis. In the homogeneous case, all elements are assigned the same material properties. In the heterogeneous case with the concrete modelled as a 3-phase composite material, each element is assigned the material properties of the phase that it represents. In the heterogeneous case with the concrete modelled as a two-phase composite material, the elements representing the aggregate and matrix phases are assigned the material properties of the aggregate and matrix phases respectively while the elements originally representing the ITZs are assigned the material properties of the matrix phase as if the ITZs have the same properties as the matrix phase. To evaluate the compressive stress-strain curves of the concrete specimens up to the post-peak range, prescribed displacements are applied to the ends of the specimen as depicted in Fig. 3(b) at smoothly applied rates as plotted in Fig. 4(b).

The stress-strain curves of the three concrete specimens so evaluated are plotted in Fig. 6. It is seen that the compressive strength of the concrete is unrealistically high when treated as a single-phase material, equal to 83.3 MPa when treated as a 3-phase composite material and equal to 110.4 MPa when treated as a two-phase composite material without ITZs. From these stress-strain curves, it is also evident that the concrete would behave in a more brittle manner when treated as a two-phase material and become very brittle when treated as a single-phase material.

The above differences in stress-strain behaviour may be explained by looking into the element stress state results. In the homogeneous case with the concrete treated as a single-phase material, all the elements fail at more or less the same time. This is the reason for the elastic-brittle failure of the concrete when treated as a single-phase material. In the heterogeneous case with the concrete treated as a 3-phase material, tension cracks initiate in the ITZs when the compressive stress at each end of the concrete specimen reaches around 7.5 MPa. At a higher stress level, the tension cracks start to propagate steadily along the ITZs and more tension cracks initiate in the other ITZs. As the stress level further increases, the tension cracks eventually propagate into the matrix phase until some of them coalesce into major cracks and finally the concrete fails. The progressive cracking of the ITZs and the matrix phase imparts strain-softening nonlinearity to the stress-strain curve and renders the failure mode of the concrete less brittle.

In the heterogeneous case with the concrete treated as a two-phase material, tension cracks initiate in the matrix phase at a much higher compressive stress level of around 25 MPa. Then as the stress level further increases, more tension cracks initiate in the matrix phase and the tension cracks formed eventually coalesce into major cracks leading to final failure of the concrete.

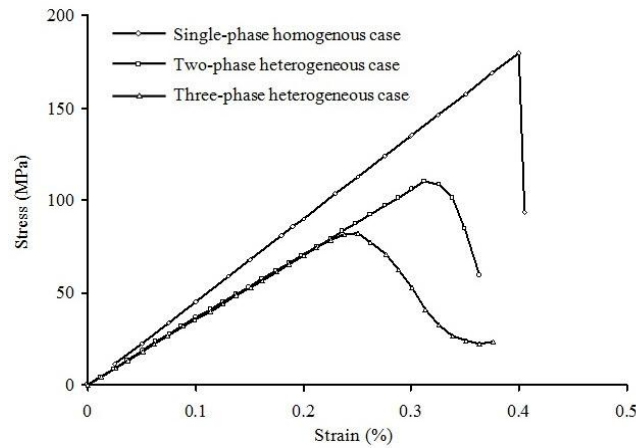


Fig. 6 Stress-strain curves of concrete under uniaxial compressive stress

Compared to the concrete treated as a 3-phase material, the failure mode is more brittle and the peak compressive stress reached is 33% higher. These differences demonstrate that the ITZs, being the weakest links in concrete, have substantial influence on the stress-strain curve and compressive strength of concrete. In particular, the observed effect of the ITZs on the compressive strength agrees quite well with the experimental results obtained by other researchers. For instance, Mindess (1996) has investigated the effects of the properties of ITZs and concluded that the compressive strength of concrete would increase by about 15 to 40% when the ITZs change from “no bond” to “perfect bond”.

### 3.4 Effects of confining stresses on failure pattern and stress-strain curve

The effects of confining stresses are investigated by analysing the concrete specimen four times under lateral confining stresses of either 0, 10, 20 or 40 MPa with the concrete treated as a 3-phase material. The same strain-softening constitutive model and the same material properties as listed in Table 1 are adopted for the analysis. During the process of load application, the lateral confining stresses together with vertical normal stresses equal to the lateral confining stresses are applied to the concrete specimen first. After then, prescribed displacements are applied to the ends of the specimen as depicted in Fig. 3(b) at smoothly applied rates as plotted in Fig. 4(b) to study the failure pattern and evaluate the deviatoric stress-strain curve of the concrete up to the post-peak range (the deviatoric stress is equal to the vertical normal stress developed at the ends of the specimen minus the lateral confining stress).

The crack propagation in the concrete under confining stresses of 0, 10, 20 and 40 MPa are depicted in Figs. 7(a), 7(b), 8(a) and 8(b), respectively. In the concrete specimen under confining stresses of 0 MPa (only uniaxial compressive stresses applied), tension cracks start to appear in the ITZs at a relatively low deviatoric stress of around 7.5 MPa. Then, as the deviatoric stress increases, more and more tension cracks initiate in the ITZs. The tension cracks eventually propagate into the matrix phase to form larger cracks, which are mostly vertical. Finally, the concrete fails by tension splitting. In the concrete specimen under confining stresses of 10 MPa, tension cracks start to appear in the ITZs at a much higher deviatoric stress of around 65 MPa.

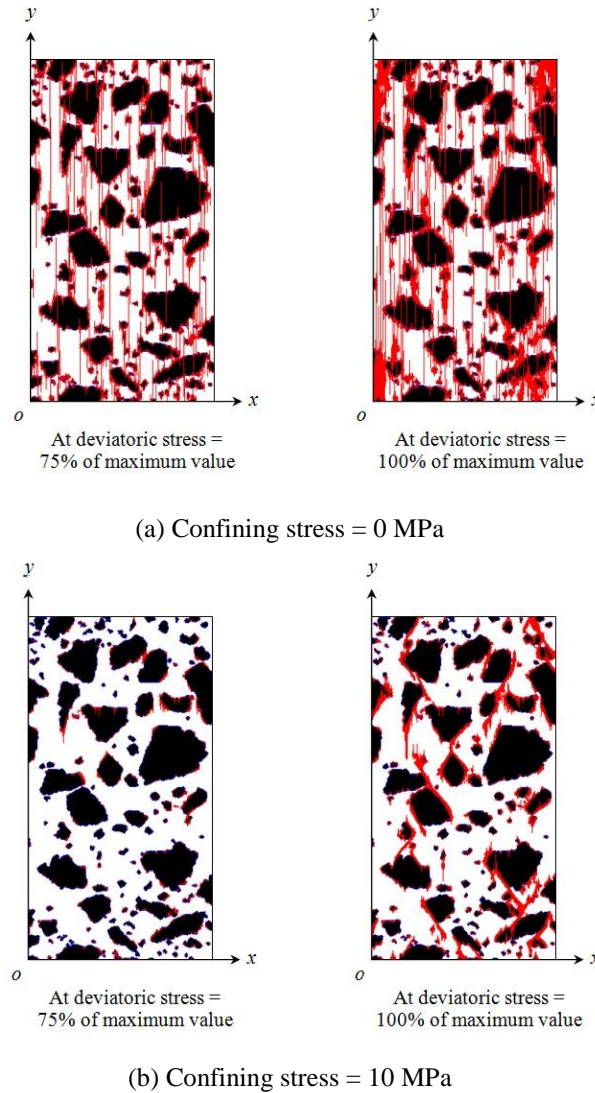


Fig. 7 Crack propagation in concrete under confining stresses of 0 and 10 MPa

Then, as the deviatoric stress increases, a few more tension cracks initiate in the ITZs. The tension cracks eventually propagate into the matrix phase to form larger cracks, which are mostly vertical. However, closer to the point of failure, shear cracks start to appear in the ITZs and some of these shear cracks propagate into the matrix phase. Finally, the concrete fails mainly by tension splitting and to a less extent by shearing. The above observed crack propagation process and failure patterns agree fairly well with the laboratory observations made by Scrivener and Pratt (1996) and Akcaoglu *et al.* (2005).

In the concrete specimen under confining stresses of 20 MPa, no crack is formed in the concrete even when the deviatoric stress reaches 75% of the maximum value. However, closer to

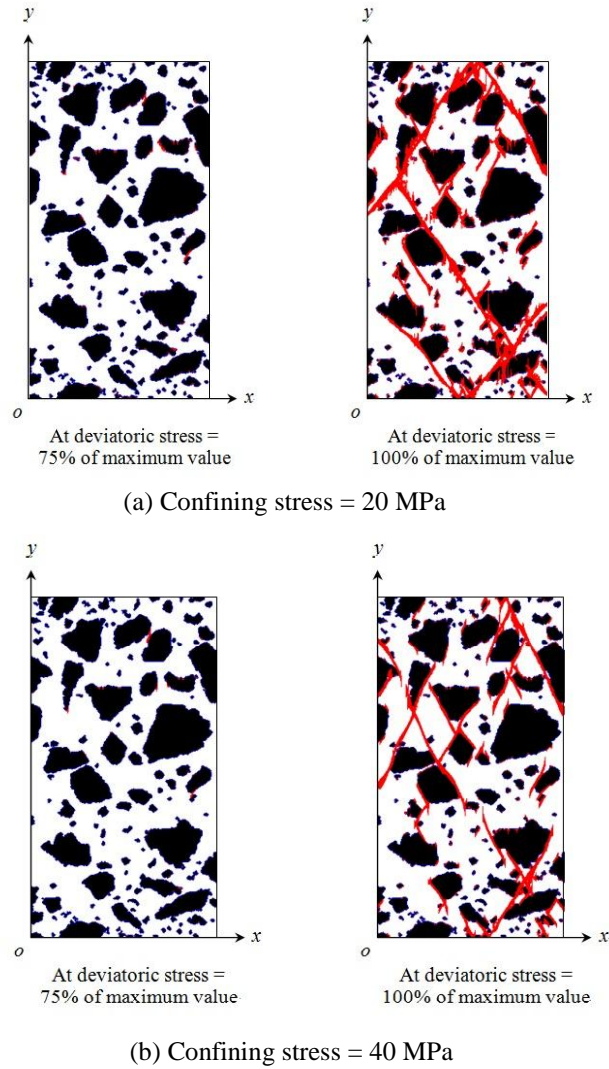


Fig. 8 Crack propagation in concrete under confining stresses of 20 and 40 MPa

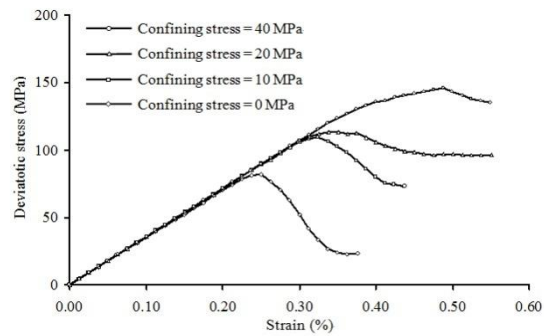


Fig. 9 Deviatoric stress-strain curves of concrete under different confining stresses

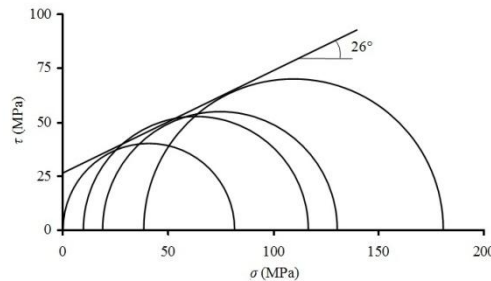


Fig. 10 Mohr circles and their envelope line

the point of failure, tension and shear cracks start to appear in the ITZs at more or less the same time and soon these tension and shear cracks propagate into the matrix phase to form larger cracks. Finally, the concrete fails by a combination of tension splitting and shearing. In the concrete specimen under confining stresses of 40 MPa, no crack is formed in the concrete even when the deviatoric stress reaches 75% of the maximum value. Closer to the point of failure, shear cracks start to appear in the ITZs and soon these shear cracks propagate into the matrix phase to form larger cracks, which are mostly inclined. Finally, the concrete fails by shearing.

The deviatoric stress-strain curves so obtained for the concrete specimens under different confining stresses are presented in Fig. 9. From these curves, it is evident that with higher confining stresses applied, both the compressive strength and ductility of the concrete would increase very substantially. Such increases in compressive strength and ductility may be attributed to the increased clamping forces against tension splitting failure and the increased frictional forces against shearing failure when the confining stresses are increased. These observations agree quite well with the laboratory test results obtained by Paterson (1978), Brady and Brown (1992) and Sheng *et al.* (2002) and the numerical simulation results obtained by Fang and Harrison (2001, 2002).

The effect of the confining stresses on the compressive strength is better illustrated by plotting the Mohr circles of the concrete under different confining stresses and the linear envelope line of the Mohr circles in Fig. 10. The intercept and slope of the envelope line are found to be 26.3 MPa and  $26^\circ$ , respectively. These are physically the cohesion and friction angle of the concrete treated as a material by itself. Comparing with the material properties of the individual phases listed in Table 1, it can be seen that the cohesion of the concrete is about the same as that of the ITZs, while the friction angle of the concrete is slightly smaller than that of the ITZs. This indicates that the mechanical properties of concrete are not simple functions of the material properties of the individual phases. The material heterogeneity causes uneven stress distribution in the concrete and complex interaction between the three individual phases, and, as a result, the mechanical properties of concrete are totally different from the weighted average values of the material properties of the individual phases. Lastly, it is noteworthy that the envelope line does not match all the Mohr circles. The exact reason is not known, although quite possibly the slight mismatch is due partly to the out-of-plane stresses induced by the plane strain condition applied and partly to numerical errors. Further investigations on the effects of the material properties of the ITZs and the combined effects of the in-plane and out-of-plane confining stresses are recommended.

#### 4. Conclusions

An actual microstructure-based numerical method for analysing the mechanical behaviour of concrete at mesoscopic level has been developed. Unlike previous numerical methods developed by others, which artificially generate the 3-phase microstructure of concrete either arbitrarily by hand or randomly by statistical tools, the method developed herein employs the digital image processing technique to capture the actual microstructure of concrete from the surfaces of real concrete for mechanical analysis. With the actual microstructure of concrete obtained by image measurement adopted in the analysis, the numerical results should be more representative of real concrete. For the mechanical analysis, the finite difference code FLAC<sup>2D</sup> is used because it remains numerically stable even when the concrete is failing in a brittle manner. However, in theory, other computer codes such as those based on the finite element method may also be used.

Numerical examples, comprising of three series of parametric studies, have been presented. The first series on the effects of heterogeneity revealed that even with a uniform uniaxial compressive stress applied in the longitudinal direction, the heterogeneity arising from the presence of different phases would cause uneven distribution of longitudinal stresses and induce both compressive and tensile lateral stresses in the concrete. The second series on the effects of interfacial transition zones indicated that the interfacial transition zones have governing effects on both the compressive strength and ductility of concrete. Finally, the third series on the effects of confining stresses showed that due to the weak bond strength of the interfacial transition zones, unconfined concrete would fail by tension splitting, but with lateral confining stresses applied, the concrete might fail with a combined tension splitting and shearing mode or even with a pure shearing mode. The increase in compressive strength with the magnitude of the confining stresses applied follows roughly the Mohr-Coulomb relation. Moreover, treated as a material by itself, concrete has a cohesion about the same as that of the interfacial transition zones and a friction angle slightly smaller than that of the interfacial transition zones. On the whole, the mesoscopic behaviour of concrete revealed in this study agrees quite well with the experimental and numerically simulated results by others.

It is noteworthy that up to now, there is no consensus on the effects of interfacial transition zones on the compressive strength of concrete. Different researchers using different approaches have obtained widely different and even contradictory results. Although many studies, including the present one, have revealed that the interfacial transition zones should have great effects on the compressive strength, some researchers (Diamond and Huang 2001; Akcaoglu *et al.* 2005) have found that the interfacial transition zones have little effects on the compressive strength. Further studies are recommended to resolve this controversial issue.

#### References

- Akcaoglu, T., Tokyay, M. and Celik, T. (2005), "Assessing the ITZ microcracking via scanning electron microscope and its effect on the failure behavior of concrete", *Cement Concrete Res.*, **35**(2), 358-363.
- Azevedo, N., May, I. and Lemos, I.J. (2002), "Numerical simulations of plain concrete under shear loading conditions", *Numerical Modeling in Micromechanics via Particle Methods - Proceedings of the 1st International PFC Symposium, Gelsenkirchen, Germany*.
- Bazant, Z.P., Tabbara, M.R., Kazemi, M.T. and Pijaudier-Cabot, G. (1990), "Random particle model for fracture of aggregate or fiber composites", *J. Eng. Mech. ASCE*, **116**(8), 1686-1705.
- Billaux, D., Detournay, C., Hart, R. and Rachez, X. (2001), "FLAC and numerical modeling in

- geomechanics”, *Proceedings of the 2nd International FLAC Symposium*, Lyon, France.
- Brady, B.H.G. and Brown, E.T. (1992), *Rock Mechanics for Underground Mining (2nd ed.)*, Chapman & Hall, London.
- Chen, S., Yue, Z.Q., Tham, L.G. and Lee, P.K.K. (2004a), “Modeling of the indirect tensile test for inhomogeneous granite using a digital image-based numerical method”, *Int. J. Rock Mech. Min. Sci.*, **41**(3), 447 (SINOROCK Paper No. 2B01 in CDROM).
- Chen, S., Yue, Z.Q. and Tham, L.G. (2004b), “Digital image-based numerical modeling method for prediction of inhomogeneous rock failure”, *Int. J. Rock Mech. Min. Sci.*, **41**(6), 939-957.
- Chermant, J.L. (2001), “Why automatic image analysis? An introduction to this issue”, *Cement Concrete Compos.*, **23**(2-3), 127-131.
- Chermant, J.L., Chermant, L., Coster, M., Dequiedt, A.S. and Redon, C. (2001), “Some fields of applications of automatic image analysis in civil engineering”, *Cement Concrete Compos.*, **23**(2-3), 157-169.
- Comby-Peyrot, I., Bernard, F., Bouchard, P.O., Bay, F. and Garcia-Diaz, E. (2009), “Development and validation of a 3D computational tool to describe concrete behaviour at mesoscale: application to the alkali-silica reaction”, *Comput. Mater. Sci.*, **46**(4), 1163-1177.
- De Schutter, G. and Taerwe, L. (1993), “Random particle model for concrete based on Delaunay triangulation”, *Mater. Struct.*, **26**(2), 67-73.
- Diamond, S. and Huang, J.D. (2001), “The ITZ in concrete - a different view based on image analysis and SEM observations”, *Cement Concrete Compos.*, **23**(2-3), 179-188.
- Fang, Z. and Harrison, J.P. (2001), “A mechanical degradation index for rock”, *Int. J. Rock Mech. Min. Sci.*, **38**(8), 1193-1199.
- Fang, Z. and Harrison, J.P. (2002), “Development of a local degradation approach to the modeling of brittle fracture in heterogeneous rocks”, *Int. J. Rock Mech. Min. Sci.*, **39**(4), 443-457.
- ITASCA (1995), *Fast Lagrangian Analysis of Continua (Version 3.3)*, Minnesota, USA.
- Kwan, A.K.H., Mora, C.F. and Chan, H.C. (1999a), “Particle shape analysis of coarse aggregate using digital image processing”, *Cement Concrete Res.*, **29**(9), 1403-1410.
- Kwan, A.K.H., Wang, Z.M. and Chan, H.C. (1999b), “Mesoscopic study of concrete II: nonlinear finite element analysis”, *Comput. Struct.*, **70**(5), 545-556.
- Liao, K.Y., Chang, P.K., Peng, Y.N. and Yang, C.C. (2004), “A study on characteristics of interfacial transition zone in concrete”, *Cement Concrete Res.*, **34**(6), 977-989.
- Leite, J.P.B., Slowik, V. and Apel, J. (2007), “Computational model of mesoscopic structure of concrete for simulation of fracture processes”, *Comput. Struct.*, **85**(17-18), 1293-1303.
- Mindess, S. (1996), “Tests to determine the mechanical properties of the interfacial zone”, *Interfacial Transition Zone in Concrete: State-of-the-Art Report prepared by RILEM Technical Committee 108-ICC, Interfaces in Cementitious Composites*, Toulouse, France.
- Mora, C.F. and Kwan, A.K.H. (2000), “Sphericity, shape factor, and convexity measurement of coarse aggregate for concrete using digital image processing”, *Cement Concrete Res.*, **30**(3), 351-358.
- Mora, C.F., Kwan, A.K.H. and Chan, H.C. (1998), “Particle size distribution analysis of coarse aggregate using digital image processing”, *Cement Concrete Res.*, **28**(6), 921-932.
- Oliver, J.P., Maso, J.C. and Bourdette, B. (1995), “Interfacial transition zone in concrete”, *Adv. Cement Based Mater.*, **2**(1), 30-38.
- Paterson, M.S. (1978), *Experimental Rock Deformation: the Brittle Field*, Springer, Berlin.
- Raghuprasad, B.K., Bhat, D.N. and Bhattacharya, G.S. (1998), “Simulation of fracture in a quasi-brittle material in direct tension - a lattice model”, *Eng. Fract. Mech.*, **61**(3-4), 445-460.
- Rempling, R. and Grassl, P. (2008), “A parametric study of the meso-scale modelling of concrete subjected to cyclic compression”, *Cement Concrete*, **5**(4), 359-373.
- Schlangen, E. and Van Mier, J.G.M. (1992), “Experimental and numerical analysis of micromechanisms of fracture of cement-based composites”, *Cement Concrete Compos.*, **14**(2), 105-118.
- Schlangen, E. and Garboczi, E.J. (1996), “New method for simulating fracture using an elastically uniform random geometry lattice”, *Int. J. Eng. Sci.*, **34**(10), 1131-1144.
- Scrivener, K.L. and Pratt, P.L. (1996), “Characterisation of interfacial microstructure”, *Interfacial Transition*

- Zone in Concrete: State-of-the-Art Report prepared by RILEM Technical Committee 108-ICC, Interfaces in Cementitious Composites, Toulouse, France.
- Sheng, Q., Yue, Z.Q., Lee, C.F., Tham, L.G. and Zhou, H. (2002), "Estimating the excavation disturbed zone in permanent shiplock slopes of the Three Gorges Project, China", *Int. J. Rock Mech. Min. Sci.*, **39**(2), 165-184.
- The MathWorks Inc. (2007), Getting Started with MATLAB® 7, Website: <http://www.mathworks.com/>.
- Wang, Z.M., Kwan, A.K.H. and Chan, H.C. (1999), "Mesoscopic study of concrete I: generation of random aggregate structure and finite element mesh", *Comput. Struct.*, **70**(5), 533-544.
- Wittmann, F.H., Roelfstra, P.E. and Sadouki, H. (1984), "Simulation and analysis of composite structures", *Mater. Sci. Eng.*, **68**(2), 239-248.
- Wriggers, P. and Moftah, S.O. (2006), "Mesoscale models for concrete: homogenisation and damage behaviour", *Finite Elements Anal. Design*, **42**(7), 623-636.
- Yue, Z.Q., Chen, S. and Tham, L.G. (2003a), "Finite element modeling of geomaterials using digital image processing", *Comput. Geo.*, **30**(5), 375-397.
- Yue, Z.Q., Chen, S. and Tham, L.G. (2003b), "Seepage analysis in inhomogeneous geomaterials using digital image processing based finite element method", *Proceedings of the 12th Panamerican Conference for Soil Mechanics and Geotechnical Engineering and the 39th US Rock Mechanics Symposium*, Soil and Rock America, Boston.
- Yue, Z.Q. and Morin, I. (1996), "Digital image processing for aggregate orientation in asphalt concrete mixtures", *Can. J. Civil Eng.*, **23**(2), 480-489.
- Zaitsev, Y.B. and Wittmann, F.H. (1981), "Simulation of crack propagation and failure of concrete", *Mater. Construct.*, **14**(5), 357-365.
- Zhu, W.C., Teng, J.G. and Tang, C.A. (2004), "Mesomechanical model for concrete. Part I: Model development", *Mag. Conc. Res.*, **56**(6), 313-330.